

The two-component X-ray spectrum of the 6.4 s pulsar 1E 1048.1–5937

T. Oosterbroek¹, A.N. Parmar¹, S. Mereghetti², and G.L. Israel³

¹ Astrophysics Division, Space Science Department of ESA, ESTEC, P.O. Box 299, 2200 AG Noordwijk, The Netherlands

² IFCTR, via Bassini 15, I-20133 Milano, Italy

³ Osservatorio Astronomico di Roma, via dell'Osservatorio 1, I-00040 Monteporzio Catone, Italy

Received 31 October 1997 / Accepted 6 March 1998

Abstract. The 6.4 s X-ray pulsar 1E 1048.1–5937 was observed by *BeppoSAX* in 1997 May. This source belongs to the class of “anomalous” pulsars which have pulse periods in range 5–11 s, show no evidence of optical or radio counterparts, and exhibit long-term increases in pulse period. The phase-averaged 0.5–10 keV spectrum can be described by an absorbed power-law and blackbody model. The best-fit photon index is 2.5 ± 0.2 and the blackbody temperature and radius are 0.64 ± 0.01 keV and 0.59 ± 0.02 km (for a distance of 3 kpc), respectively. The detection of blackbody emission from this source strengthens the similarity with two of the more well studied “anomalous” pulsars, 1E 2259+586 and 4U 0142+614. There is no evidence for any phase dependent spectral changes.

The pulse period of 6.45026 ± 0.00001 s implies that 1E 1048.1–5937 continues to spin-down, but at a slower rate than obtained from the previous measurements in 1994 and 1996.

Key words: stars: neutron – pulsars: individual (1E 1048.1–5937) – X-rays: stars

1. Introduction

1E 1048.1–5937 is an unusual pulsar, with a period of 6.4 s and a soft spectrum, discovered during *Einstein* observations of the Carina nebula (Seward et al. 1983). The source has been spinning down for at least the last 17 years (Mereghetti 1995; Corbet & Mihara 1997). The spectrum has been modeled by an absorbed power-law with a photon index, α , of ~ 2 –3 (Seward et al. 1983; Corbet & Mihara 1997). This spectral shape is softer than those of typical high-luminosity X-ray pulsars. Despite a small error box, no optical counterpart has been identified, with a limiting magnitude of $m_V \sim 20$ which excludes the presence of a massive companion (Mereghetti et al. 1992). A recent observation with the *RossixTE* satellite provides a strong upper limit to the projected X-ray semi-major axis of 0.06 lt-s for orbital periods between 200 s and ~ 1 day (Mereghetti et al. 1997). The lack of an optical counterpart and orbital Doppler shifts argue against a binary model for 1E 1048.1–5937, unless

the companion has a low mass. Mereghetti et al. (1997) find that a probable upper limit to the mass of a Roche lobe filling main sequence companion is $\sim 0.3 M_\odot$. Masses up to $\sim 0.8 M_\odot$ are allowed in the case of a helium-burning companion filling its Roche lobe.

The properties described above are similar to those of a small number of other X-ray pulsars with spin periods in the 5–11 s range (Mereghetti & Stella 1995), such as 1E 2259+586 and 4U 0142+614. These form a class of so-called “anomalous” pulsars, with clearly different properties from the majority of systems. Although accretion from a very low mass companion cannot be excluded, the lack of evidence for a binary nature from any of these systems has stimulated models where the X-ray emission originates from a compact object that is not in an interacting binary system. While an isolated, massive, white dwarf powered by the loss of rotational energy, as originally proposed for 1E 2259+586 (Paczynski 1990; Usov 1994), has been ruled out by the detection of a large increase in the spin-down rate of 1E 1048.1–5937 (Mereghetti 1995), other single object models, such as loss of magnetic energy of a strongly magnetized neutron star (Thompson & Duncan 1993), or an isolated neutron star accreting from a circumstellar disk (Corbet et al. 1995; van Paradijs et al. 1995), may be applicable.

We present a study of 1E 1048.1–5937 based on data obtained with the *BeppoSAX* satellite. We focus on the X-ray spectrum at energies < 10 keV and on the pulse period history. As with some of the other “anomalous” pulsars, we find evidence for the presence of a blackbody spectral component. Since this component is not observed from the majority of other accreting X-ray pulsars, this strengthens the similarity between 1E 1048.1–5937 and the other better studied “anomalous” pulsars.

2. Observations

Results were obtained with the Low-Energy Concentrator Spectrometer (LECS; 0.1–10 keV; Parmar et al. 1997a) and Medium-Energy Concentrator Spectrometer (MECS; 1.3–10 keV; Boella et al. 1997) instruments. The MECS consists of three identical grazing incidence telescopes with imaging gas scintillation proportional counters in their focal planes. The LECS uses an identical telescope as the MECS, but utilizes an ultra-thin ($1.25 \mu\text{m}$)

Send offprint requests to: T. Oosterbroek: toosterb@astro.estec.esa.nl

Table 1. Spectral fit results for 1E 1048.1–5937. Uncertainties are given at 68% confidence for one parameter of interest. The normalization is at 1 keV

Parameter	Value
power-law model	
α	3.36 ± 0.05
N_{H} (10^{22} atoms cm^{-2})	1.54 ± 0.10
χ^2_{ν} (dof)	1.520 (304)
power-law & blackbody model	
α	2.52 ± 0.20
kT_{bb} (keV)	0.64 ± 0.01
R_{bb}^a (km)	0.59 ± 0.02
N_{H} (10^{22} atoms cm^{-2})	0.45 ± 0.10
χ^2_{ν} (dof)	0.997 (302)
Broken power-law model	
α_1	1.71 ± 0.2
α_2	3.58 ± 0.08
Break Energy (keV)	1.71 ± 0.2
N_{H} (10^{22} atoms cm^{-2})	0.47 ± 0.07
χ^2_{ν} (dof)	1.015 (302)
Two blackbody model	
$kT_{\text{bb}1}$ (keV)	0.58 ± 0.02
$R_{\text{bb}1}^a$ (km)	0.77 ± 0.08
$kT_{\text{bb}2}$ (keV)	1.25 ± 0.12
$R_{\text{bb}2}^a$ (km)	0.10 ± 0.03
N_{H} (10^{22} atoms cm^{-2})	0.14 ± 0.04
χ^2_{ν} (dof)	0.964 (302)
Cut-off power-law model	
α	0.42 ± 0.07
Cut-off energy (keV)	1.43 ± 0.13
N_{H} (10^{22} atoms cm^{-2})	0.42 ± 0.07
χ^2_{ν} (dof)	1.041 (303)

^aFor a distance of 3 kpc

entrance window and a driftless configuration to extend the low-energy response to 0.1 keV. The fields of view of the LECS and MECS are circular with diameters of 37' and 56', respectively. In the overlapping energy range, the position resolution of both instruments is similar and corresponds to 90% encircled energy within a radius of 2.5' at 1.5 keV. At lower energies, the encircled energy is proportional to $E^{-0.5}$. In the central 10' the LECS 0.1–10 keV and the MECS 1–11 keV background counting rates are 9.7×10^{-5} arcmin $^{-2}$ s $^{-1}$ and 10.9×10^{-5} arcmin $^{-2}$ s $^{-1}$ (for 2 MECS units), respectively.

1E 1048.1–5937 was observed by *BeppoSAX* on 1997 May 10 01^h 24^m to May 11 15^h 24^m UTC. Good data were selected from time intervals when the minimum elevation angle above the Earth's limb was $>4^\circ$ and when the instrument configurations were nominal using the SAXDAS 1.2.0 data analysis package. This gives exposures of 80 ks for the MECS and 32 ks for the LECS, which was only operated during satellite night-time. One of the three MECS units failed on 1997 May 9 (one day before our observation), and data were only obtained from the remaining two MECS units.

3. Results

3.1. Spectral analysis

Spectra were obtained centered on the pulsar position using extraction radii of 8' and 4' for the LECS and MECS, respectively. The appropriate LECS response matrix was generated using LEMAT 3.4.0. Background subtraction was performed using standard blank field exposures. The background subtracted 1E 1048.1–5937 count rates are 0.08 and 0.12 s $^{-1}$ in the LECS and MECS, respectively. Examination of the LECS spectrum reveals that the pulsar is only detected above 0.5 keV, and data below this energy are excluded. Similarly, the MECS fits are restricted to the energy range 1.65–10 keV. All the spectra were rebinned to have >20 counts in each bin to allow the use of χ^2 statistics.

In order to compare our results with previous observations, the spectra were first fit with two models: (i) an absorbed power-law, and (ii) an absorbed power-law plus blackbody. Although a single power-law with $\alpha=4.04$ satisfactorily describes the MECS spectrum, it is clearly inadequate when the LECS spectrum is included, giving a χ^2_{ν} of 1.520 for 304 degrees of freedom (dof). Figure 1 shows the fit residuals before and after the inclusion of the blackbody component. The power-law plus blackbody model gives a χ^2_{ν} of 0.997 for 302 dof for a blackbody temperature, kT_{bb} , of 0.64 ± 0.01 keV and radius, R_{bb} , of 0.59 ± 0.02 km for a distance of 3 kpc. The best-fit value of α is 2.52 ± 0.20 and low-energy absorption, N_{H} , equivalent to $(4.5 \pm 1.0) \times 10^{21}$ atoms cm^{-2} is required. An F-test shows that the inclusion of the blackbody is highly significant (the reduction in χ^2 has a formal probability of $\sim 10^{-28}$, corresponding to $\sim 11\sigma$). The best fit two-component spectrum is plotted in Fig. 1 and the corresponding parameters are given in Table 1. The unabsorbed 2–10 keV source flux is 7.0×10^{-12} ergs cm^{-2} s $^{-1}$, with the blackbody component accounting for 55% of the flux in this energy range. For comparison, the results of fitting the same spectral model to some other “anomalous” pulsars are given in Table 4. In order to investigate whether other simple spectral models can also give acceptable representations of the 1E 1048.1–5937 spectrum, fits using three additional models were also performed (see Table 1). All these models gave fits of comparable quality as the power-law and blackbody combination. This means that we are unable to meaningfully distinguish between the different spectral models listed in Table 1, with the exception of the power-law. However, in order to compare our results with previous ones, we will use power-law and blackbody fits in the subsequent analysis.

3.2. Pulse timing and phase resolved spectroscopy

The MECS counts were used to determine the 1E 1048.1–5937 pulse period, after correction of their arrival times to the solar system barycenter. The data were divided into 10 time intervals (each with ~ 950 counts) and for each interval the relative phase of the pulsations determined. The phases of the 10 time intervals were then fit with a linear function giving a best-fit period of 6.45026 ± 0.00001 s. This value is plotted together with the

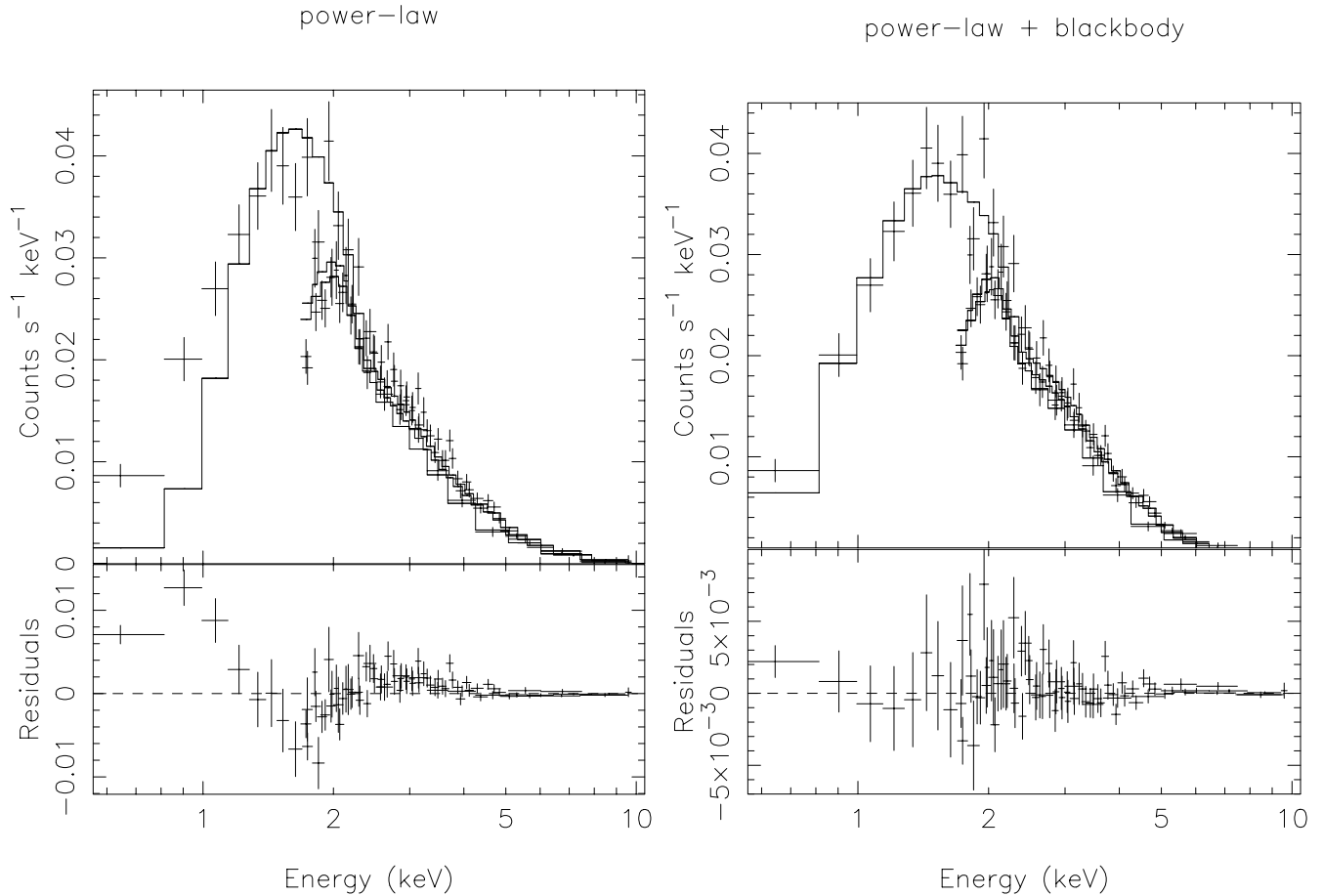


Fig. 1. The spectrum of 1E 1048.1–5937 obtained with the LECS and two MECS units. The left panels show the spectrum and the absorbed power-law model fit. Note the large residuals below 1.5 keV. The right panels show the spectrum with the absorbed power-law plus blackbody model fit. The units of the residuals are counts $\text{s}^{-1} \text{keV}^{-1}$

previous measurements in Fig. 3. The 0.5–10 keV folded light curve of 1E 1048.1–5937 shows an approximately sinusoidal variation with an amplitude of $\sim 70\%$ (Fig. 2). The pulsed fraction as a function of energy was determined in the following way: The data for each energy range was folded at the best-fit period and fit with a model consisting of a constant, C , and a sine term ($f(\phi) = C + A \sin(\phi + \phi_0)$). The only free parameters in this fit are C and the amplitude of the sine, A , since ϕ_0 was determined from the total energy range data and was fixed during the fits (there is no evidence for a change of ϕ_0 with energy). We then determined the pulsed fraction defined as the amplitude of the sine term (A) divided by C (a correction for background was applied). The results are given in Table 2. The correction for background is only important in the highest energy range. From this table we conclude that the pulsed fraction is approximately constant over the whole energy range. We caution that the systematic errors are largest in the highest energy bin (with the background contributing 33% of the mean count rate).

A set of 4 phase-resolved spectra of the pulsar were accumulated. These were then fit with the power-law plus blackbody model used in Sect. 3.1, with N_{H} fixed at the phase-averaged

Table 2. The pulsed fraction as a function of energy as determined from the MECS data

Energy Range (keV)	Pulsed Fraction (background corrected)
1.0–1.5	0.76 ± 0.08
1.5–2.0	0.74 ± 0.05
2.0–2.5	0.77 ± 0.04
2.5–4.0	0.84 ± 0.03
4.0–6.0	0.79 ± 0.05
6.0–10.0	0.54 ± 0.12

best-fit value. There are insufficient counts to simultaneously constrain both the power-law and blackbody components. Initially, the blackbody spectral parameters were fixed at their phase-averaged best-fit values and only the power-law parameters were allowed to vary. The resulting fits are unacceptable, primarily because the spectra obtained at the valleys are not well fit ($\chi^2_{\nu} = 2.2$ for 79 dof) due to the fixed blackbody component contributing too much flux. The fits were then repeated with the blackbody normalization allowed to vary, giving acceptable values of χ^2_{ν} (second panel of Fig. 4).

Table 3. The period history for 1E 1048.1–5937

Time (JD-2440000)	Period (s)	\dot{P}^a $10^{-4} \text{ s yr}^{-1}$	Pulsed Fraction	Observatory	Reference
4068.7	6.4377 ± 0.001	...	0.68 ± 0.07	<i>Einstein</i>	Seward et al. (1986)
6236.6	6.4407 ± 0.0009	5 ± 2	0.68	EXOSAT	Seward et al. (1986)
7267.0	6.44153 ± 0.0002	...		<i>Ginga</i>	Corbet & Day (1990)
7277.0	6.44185 ± 0.00001	4 ± 3	... ^b	<i>Ginga</i>	''
7433.0	6.4422 ± 0.0004	...		<i>Ginga</i>	''
8787.24	6.444868 ± 0.000007	7.29 ± 0.03	~ 0.70	ROSAT	Mereghetti (1995)
8844.48	6.44499 ± 0.000034	...		ROSAT	''
8972.74	6.44532 ± 0.000072	...		ROSAT	''
8994.80	6.445391 ± 0.000013	...		ROSAT	''
9417.0	6.446645 ± 0.000001	10.30 ± 0.04	0.70 ± 0.05^c	ASCA	Corbet & Mihara (1997)
10294.5	6.449769 ± 0.000004	12.99 ± 0.02	... ^d	<i>RossixTE</i>	Mereghetti et al. (1997)
10579.31	6.45026 ± 0.000013	6.3 ± 0.2	0.76 ± 0.02	<i>BeppoSAX</i>	This paper (see also Table 2)

^a The values of \dot{P} are calculated by comparing the best pulse period determined by each satellite with respect to that of the previous one, i.e. a long term average.

^b No value for the pulsed fraction is reported for the *Ginga* observation due to source confusion.

^c Obtained from Fig. 2 in Corbet & Mihara (1997)

^d Not reported.

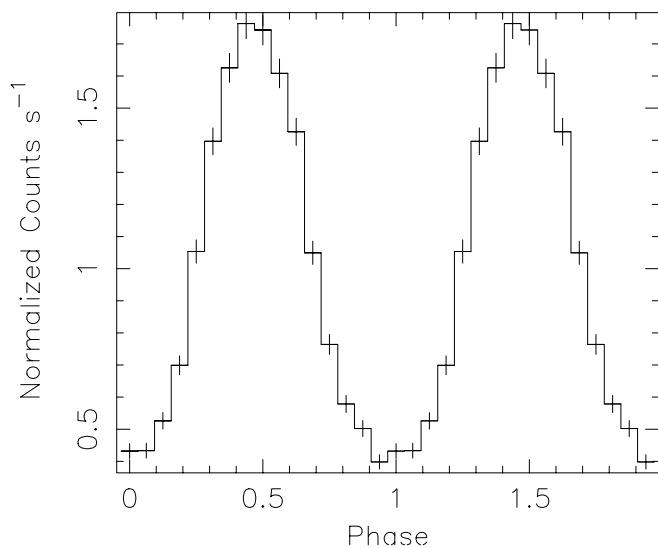


Fig. 2. The 0.5–10 keV pulse profile of 1E 1048.1–5937. For clarity, the pulse profile is repeated

The best-fit values of α obtained with a variable blackbody normalization are shown in Fig. 4 (bottom panel) and reveal a marginal phase dependence (χ^2 of 11.1 for 3 dof, corresponding to the 1% level). A phase dependence of the blackbody radius is evident. The variation in α may be caused by inadequacies in the model, or correlations between the derived fit-parameters. The phase-resolved spectra were also fit with both α and kT_{bb} fixed and both normalizations free. This also gives acceptable values of χ^2_{ν} which are almost identical to those obtained from the fit described above. The derived blackbody radii are not significantly different from those obtained with the variable power-law index fits (see Fig. 4). We conclude that there is no evidence for any phase dependent changes in either α or kT_{bb} .

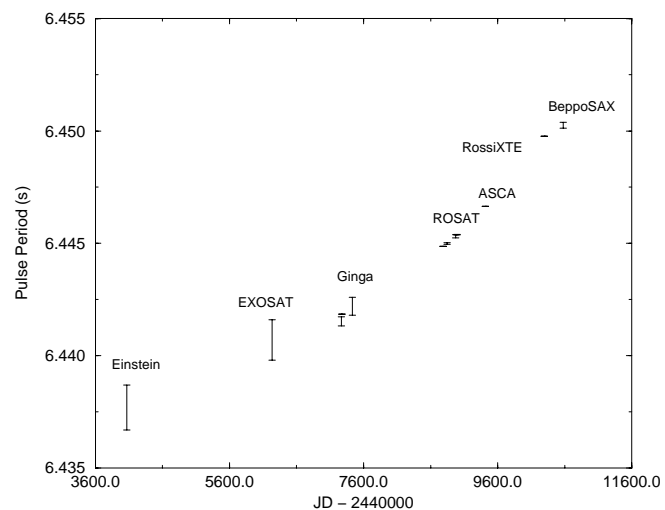


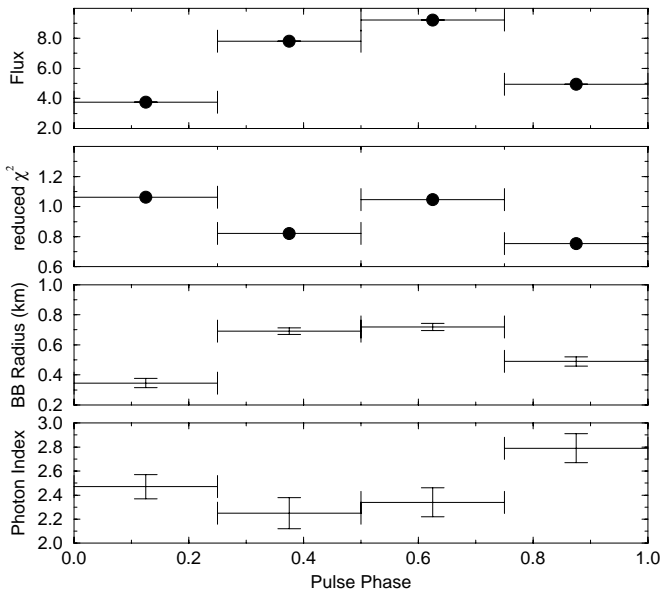
Fig. 3. The pulse period of 1E 1048.1–5937 as a function of time. Data have been obtained from Mereghetti (1995), Corbet & Mihara (1997) and Mereghetti et al. (1997)

4. Discussion

The 0.5–10 keV spectrum of 1E 1048.1–5937 can be described by the sum of an absorbed power-law and blackbody models. The existence of a blackbody component in 1E 1048.1–5937 was first suggested by the ASCA results of Corbet & Mihara (1997). However, these authors are unable to clearly discriminate between this two component model, which gives a χ^2_{ν} of 0.94 for 332 dof, and an absorbed power-law which also provides an acceptable description of the ASCA data with a χ^2_{ν} of 1.02 for 337 dof. The *BeppoSAX* results reported here clearly require that the 1E 1048.1–5937 spectrum differs significantly from an absorbed power-law. This deviation is consistent with a blackbody, but we cannot exclude the possibility that it has

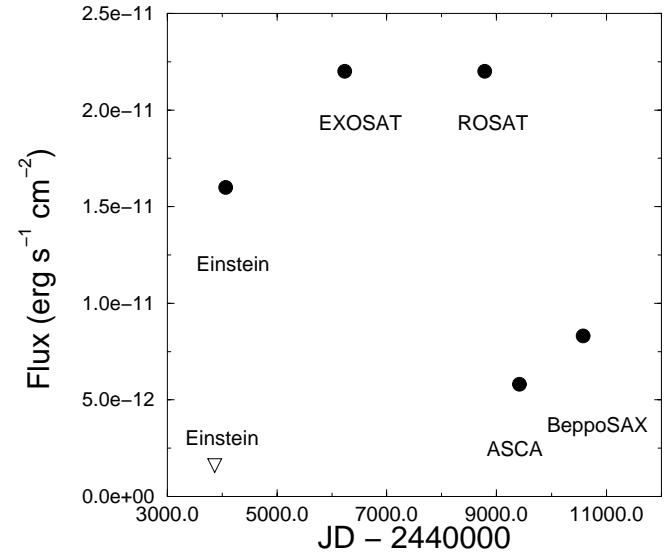
Table 4. The parameters of the “anomalous” pulsars

Source	P (s)	kT_{bb} (keV)	R_{bb} (km)	$\frac{L_{\text{bb}}}{L_{\text{tot}}}$	α	f_{pulse}^a	References
4U 0142+61	8.69	0.39	$2.4d_{1\text{kpc}}$	0.4	3.67 ± 0.09	$\sim 10\%$	White et al. (1996)
RX J0720.4-3125 ^b	8.38	0.079 ± 0.004^c	Haberl et al. (1996)
1E 1048-5937	6.45	0.64 ± 0.01	$0.59\pm 0.02 d_{3\text{kpc}}$	0.55	2.5 ± 0.2	$\sim 70\%$	
1RXS J170849.0-400910	11.00	0.41 ± 0.03	$4\pm 0.6 d_{10\text{kpc}}$	0.17	2.9 ± 0.3	$\sim 30\%$	Sugizaki et al. (1997)
1E 1841-045	11.77	3.0 ± 0.2	$\sim 35\%$	Vasisht & Gotthelf (1997)
1E 2259+586	6.98	0.44 ± 0.01	$3.3\pm 0.3 d_{4\text{kpc}}$	0.4	3.93 ± 0.09	$\sim 30\%$	Corbet et al. (1995); Parmar et al. (1997b)

^a Amplitude of pulsed emission^b Membership of “anomalous” pulsar class uncertain^c Obtained from one component blackbody fit**Fig. 4.** Spectral fit parameters as a function of pulse phase. Errors are at 68% confidence for 1 parameter of interest. The blackbody radius is for an assumed distance of 3 kpc, the flux in the top-panel is in units of 10^{-12} ergs s^{-1} cm^{-2} . Pulse phase is the same as in Fig. 2

another form. A discussion about the physical interpretation of the alternate models can be found in White et al. (1996). This discussion is applicable to 1E 1048.1–5937, since its spectral shape is roughly similar to that of 4U 0142+614. The reason for the significant *BeppoSAX* detection of spectral complexity is probably related to the combination of good energy resolution and extended low energy coverage of the LECS, together with the longer *BeppoSAX* exposure.

1E 2259+586 (Corbet et al. 1995) and 4U 0142+614 (White et al. 1996) have also been successfully fit with absorbed power-law and blackbody spectral models. Since the majority of X-ray pulsar spectra are fit by absorbed power-law models in the 0.5–10 keV energy range (e.g., White et al. 1983), our results strengthen the similarity between 1E 1048.1–5937 and the other “anomalous” pulsars. Table 4 is a compilation of the spectral properties of these “anomalous” pulsars. The blackbody component in these systems has been interpreted as evidence for

**Fig. 5.** The 2–10 keV flux of 1E 1048.1–5937 as a function of time. Data are from Seward et al. (1986), Mereghetti (1995) and Corbet & Mihara (1997). The ASCA and *BeppoSAX* values are for a power-law fit (to be consistent with the other measurements); the values obtained with 2-component fits are $\sim 15\%$ lower. The first point (open triangle) is the upper limit reported in Seward et al. (1986), where a short discussion about the uncertainties in this value can be found. ROSAT and *Einstein* fluxes in the 2–10 keV band are taken from Mereghetti (1995) and Seward et al. (1986)

quasi-spherical accretion onto an isolated neutron star formed after common envelope evolution and spiral-in of a massive X-ray binary (White et al. 1996). In this case, the accretion flow results from the remaining part of the massive star’s envelope and may consist of two components (Ghosh et al. 1997). A low-angular momentum component gives rise to the blackbody emission from a considerable fraction of the neutron star surface, while a high-angular momentum component forms an accretion disk and is responsible for the power-law emission and the long term spin-down evolution.

The area for the blackbody emitting surface obtained for 1E 1048.1–5937 ($\sim 0.59 d_{3\text{kpc}}$ km) is smaller than those of the other “anomalous” systems. However, the distance to

1E 1048.1–5937 is poorly constrained and the assumed distance of 3 kpc could be considered as a lower limit since the measured N_{H} implies that it lies behind the Carina Nebula at 2.8 kpc (Seward et al. (1986). White et al. (1996) propose that the low pulsed fraction observed from 4U 0142+614 results from the large polar cap area in this system. This is consistent with the small polar cap area and high pulsed fraction reported here for 1E 1048.1–5937 but not with 1E 2259+586 and 1RXS J170849.0–400910, which both have large radii and a moderate pulsed fraction (see Table 4). Interestingly, the best-fit blackbody temperature of 0.64 keV is somewhat higher than for 1E 2259+586 and 4U 0142+614 which may be related to the smaller area of the polar caps. Summarizing, we find that for 1E 1048.1–5937 (i) the blackbody temperature is higher, (ii) the blackbody radius is smaller, (iii) the power-law index is smaller (i.e. the spectrum is harder), and (iv) the pulsed fraction is higher than for the other “anomalous” pulsars (with the exception of RX J0720.4–3125 where the blackbody parameters are obtained from a one component fit).

The phase-resolved spectra are not well fit with a constant contribution from the blackbody component. This is unsurprising given the large pulse amplitude ($\sim 70\%$), together with the large blackbody contribution (55%; 2–10 keV) to the phase averaged flux. The probable constancy of the pulsed fraction over the 1–10 keV energy range and the lack of any spectral dependence on pulse phase (see Sect. 3.2) imply that the *whole* spectrum is varying in a similar manner; i.e. the pulsed component cannot be attributed solely to either the blackbody or the power-law components. Furthermore, the long term variations in source flux (Fig. 5) and the approximate constancy of the pulsed fraction (Table 3) during this time again implies that either the luminosities of the two components are correlated, or that the underlying spectral shape is a more complex “single component” that happens to mimic a power-law and a blackbody.

The spin-down rate of 1E 1048.1–5937 obtained from ROSAT and ASCA observations (Mereghetti 1995; Corbet & Mihara 1997), showed an 80% increase with respect to the value of $\sim 5 \times 10^{-4} \text{ s yr}^{-1}$ measured before 1988 with *Ginga* and EXOSAT. This increasing trend was further extended by the *RossixTE* observation of 1996 July ($P = 6.449769 \pm 0.000004 \text{ s}$, Mereghetti et al. 1997), yielding a \dot{P} of $13 \times 10^{-4} \text{ s yr}^{-1}$ after the ASCA measurement. The pulse period obtained with *BeppoSAX* lies significantly below the linear extrapolation from the previous two measurements, indicating, for the first time in 1E 1048.1–5937, a decrease in the overall spin-down rate.

Table 3 and Fig. 5 indicate that there is no clear correlation between the observed long term spin-down rate (\dot{P}) and the 2–10 keV source flux. At first sight this argues against an accretion hypothesis, but since \dot{P} is a long-term average and the flux an instantaneous measurement this comparison may not be valid. A much better comparison would be between the average flux and \dot{P} during the same time interval. Unfortunately, due to the faintness of the source, no such comparison is available. In view of the uncertainties in the average flux a good measure of the

time variability of the source on timescales of months to years would be useful.

Acknowledgements. The *BeppoSAX* satellite is a joint Italian–Dutch programme. T. Oosterbroek acknowledges an ESA Fellowship. We thank the staff of the *BeppoSAX* Science Data Center for their support. We thank R. Corbet for discussions and the anonymous referee for helpful suggestions.

References

- Boella G., Chiappetti L., Conti G., et al., 1997, *A&AS* 122, 327
 Corbet R.H.D., Day C.S.R., 1990, *MNRAS* 243, 553
 Corbet R.H.D., Mihara T., 1997, *ApJ* 475, L127
 Corbet R.H.D., Smale A.P., Ozaki M., Koyama K., Iwasawa K., 1995, *ApJ* 443, 786
 Ghosh P., Angelini L., White N.E., 1997, *ApJ* 478, 713
 Haberl, F., Pietsch W., Motch C., Buckley D.A.H., 1996, *IAU Circ.* 6445
 Mereghetti S., 1995, *ApJ* 455, 598
 Mereghetti S., Stella L., 1995, *ApJ* 442, L17
 Mereghetti S., Caraveo P., Bignami G.F., 1992, *A&A* 263, 172
 Mereghetti S., Israel G.L., Stella L., 1997, *MNRAS* in press
 Paczynski B., 1990, *ApJ* 365, L9
 Parmar A.N., Martin D.D.E., Bavdaz M., et al., 1997a, *A&AS* 122, 309
 Parmar A.N., Oosterbroek T., Favata F., et al., 1997b, *A&A* 330, 175
 Seward F.D., Charles P.A., Smale A.P., 1986, *ApJ* 305, 814
 Sugizaki M., Nagase F., Torii K., et al., 1997, *PASJ* 49, L25
 Thompson C., Duncan R.C., 1993, *ApJ* 408, 194
 Usov V.V., 1994, *ApJ* 427, 984
 Van Paradijs J., Taam R.E., van den Heuvel E.P.J., 1995, *A&A* 299, L41
 Vasisht G., Gotthelf E.V., 1997, *ApJ* 486, L29
 White N.E., Swank J.H., Holt S.S., 1983, *ApJ* 270, 711
 White N.E., Angelini L., Ebisawa K., Tanaka Y., Ghosh P., 1996, *ApJ* 463, L83